Supporting Information

Dual modulation on morphology and electric conductivity of NiCoP on nickel foam by Fe doping as a superior stability electrode for high energy supercapacitor

Xinwei Chang [a], Tingting Liu [b], Weilong Li [*a], Mi He [a], Zhaoyu Ren [*a], Jintao Bai [a]

[a] Institute of Photonics and Photon-Technology, Northwest University, Xi'an 710069, China

[b] School of Optoelectronic Science and Engineering, Soochow University, Suzhou 215006, China

*Corresponding authors

Prof. Weilong Li, E-mail: lwl@nwu.edu.cn

Prof. Zhaoyu Ren, E-mail: rzy@nwu.edu.cn

Experimental

(1) Synthesis of free-standing Fe doped NiCoP hierarchical nanoarrays on NF

All reagents in this experiment were of analytical grade and used without further purification. Firstly, NF (dimensions of 1*1.8 cm, areal density of 37.7 mg cm^{-2}) was rinsed via HCl and deionized (DI) water for 10 min to wipe off exterior oxides and impurities, respectively. 1 mmol of $Ni(NO_3)_2•6H_2O$, 1 mmol of $Co(NO_3)_2•6H_2O$, 3.5 mmol of NH_4F, 6.5 mmol of urea and $Fe(NO_3)_3•9H_2O$ with different molar mass (0.08 mmol, 0.125 mmol, 0.25 mmol, 0.5 mmol) were mingled in 30 ml of DI water and stirred to gain the homogeneous solution. Then the above solution and preprocessed NF were put into a Teflon-lined autoclave with the capacity of 50 mL for hydrothermal reaction at 120 °C for 6 h. Subsequently, the products were rinsed with DI water several times and dried at 60 °C overnight, and the samples were denoted as Fe-NiCo-precursor/NF-x% (x represents the feeding molar ratio of iron to the sum of cobalt and nickel, x=4, 6.25, 12.5, 25, respectively). The corresponding precursor powders were centrifugated and gathered, and the products were denoted as Fe-NiCo-precursor-x% (x=4, 6.25, 12.5, 25, respectively). Finally, the phosphorization process was executed in a quartz tube reactor heated by the horizontal furnace. The $NaH_2PO_2•H_2O$ powder and Fe-NiCo-precursor/NF-x% (Fe-NiCo-precursor-x% powder) were located in the upstream and downstream sides of the gas flow, respectively. The horizontal furnace was tardily heated to 400 °C for 2 h under the protection of Ar atmosphere. The phosphatized samples were collected after the horizontal furnace was cooled to ambient temperature naturally. The as-fabricated samples were named as Fe-NiCoP/NF-x% and

Fe-NiCoP-x% powders (x=4, 6.25, 12.5, 25), respectively. For comparison, the NiCoP/NF (NiCoP powders) was fabricated by the same steps as the synthesis procedure of Fe-NiCoP/NF-x% (Fe-NiCoP-x%) in the absence of $Fe(NO_3)_3 \cdot 9H_2O$.

(2) Material characterization

The composition and chemical valence states of samples were characterized through powder X-ray diffraction (XRD, Bruker D8 ADVANCE) and X-ray photoelectron spectrometer (XPS, VG ESCA Lab220I-XL). The morphology and structure of samples were investigated via scanning electron microscopy (SEM, Carl Zeiss SIGMA) and transmission electron microscopy (TEM, Tecnai G2 F20 S-Twin microscopy) equipped with energy-dispersive X-ray spectrometer (EDS).

(3) Electrochemical measurement

The electrochemical performance of as-synthesized electrode materials was measured via an electrochemical workstation (CHI 660D, Chenhua, Shanghai) in a three-electrode system. The as-obtained electrodes were employed directly as the working electrode, the platinum plate electrode and standard Hg/HgO electrode were acted as the counter and reference electrode, respectively. 2 M KOH aqueous solution was used as the electrolyte.

The ASC was assembled with the Fe-NiCoP/NF-12.5% and AC/NF as the positive and negative electrodes, respectively, and labeled as Fe-NiCoP/NF-12.5%//AC ASC. 2 M KOH aqueous solution was used as the electrolyte. The AC/NF electrode was fabricated by mixing the AC, polytetrafluoroethylene and acetylene black (weight ratio of 8:1:1) in N-methlpyrrolidone and painted onto NF, followed dried at 80 °C

overnight.

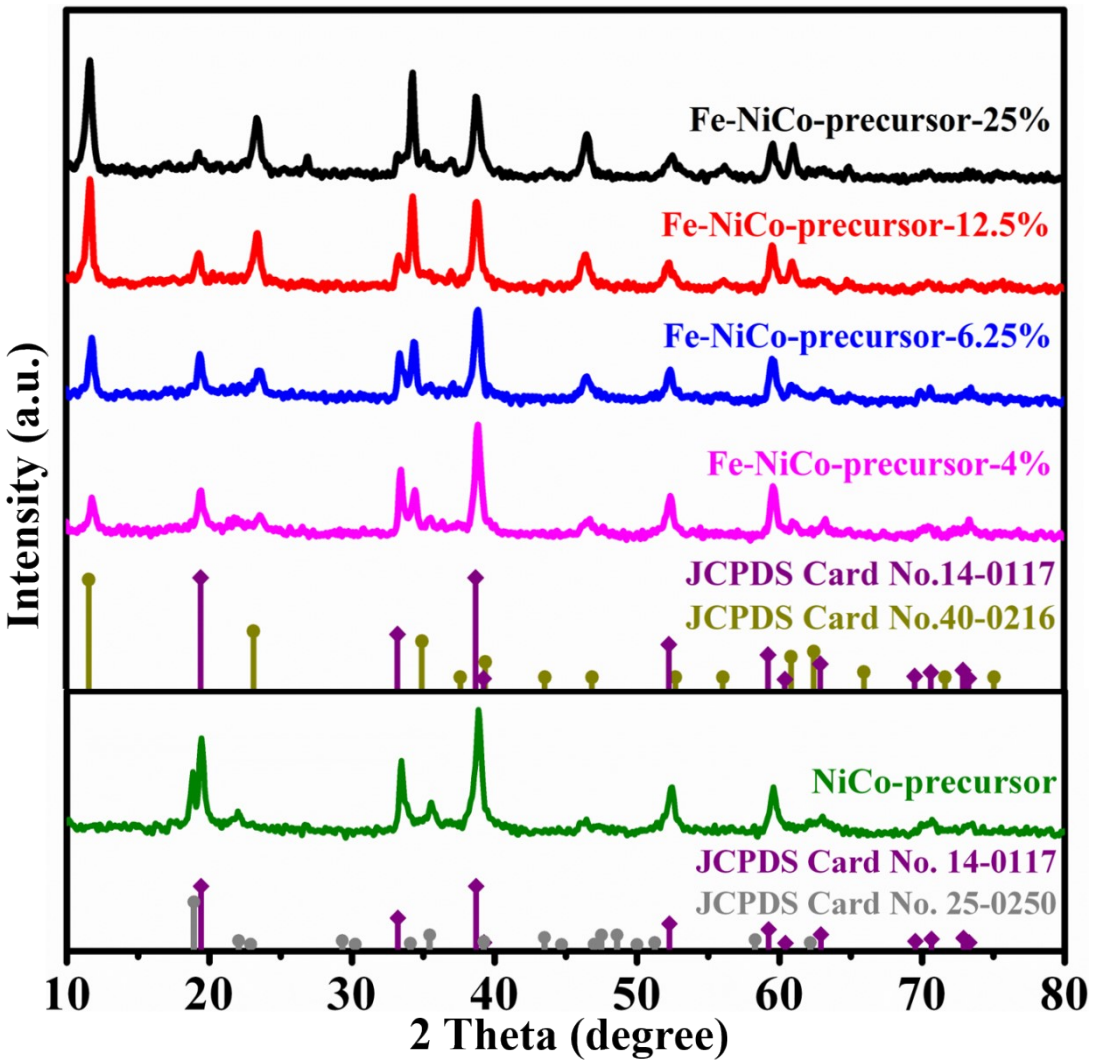

Fig. S1 XRD patterns of NiCo-precursor powder and Fe-NiCo-precursor-x% powder samples.

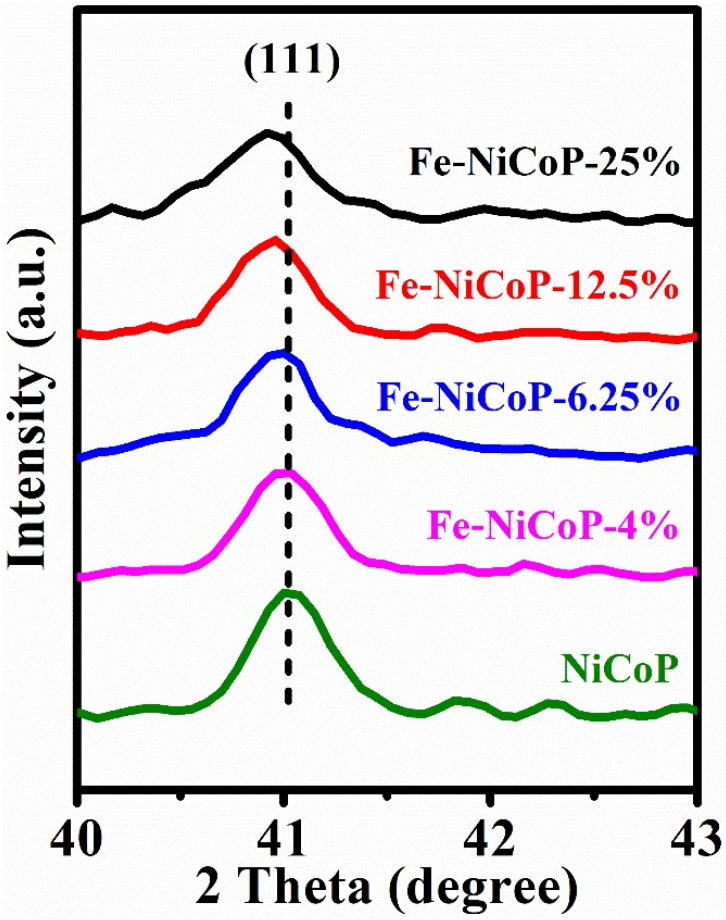

Fig. S2 Amplified XRD patterns of NiCoP powder and Fe-NiCoP-x% powder samples.

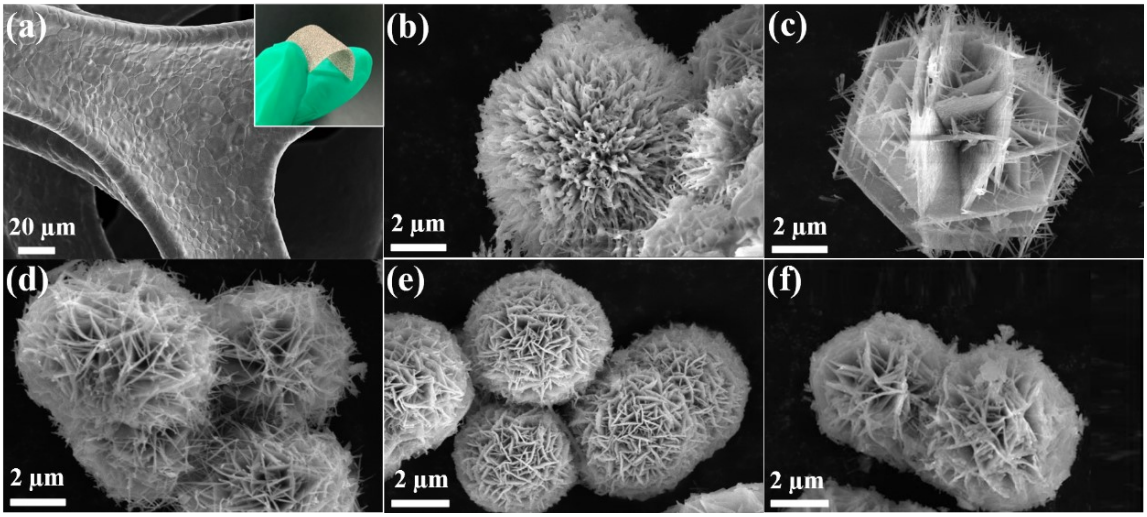

Fig. S3 (a) SEM image of nickel foam. Inset shows the Optical micrograph of the flexible nickel foam. (b-f) SEM image of NiCoP powder, Fe-NiCoP-4% powder, Fe-NiCoP-6.25% powder, Fe-NiCoP-12.5% powder and Fe-NiCoP-25% powder samples.

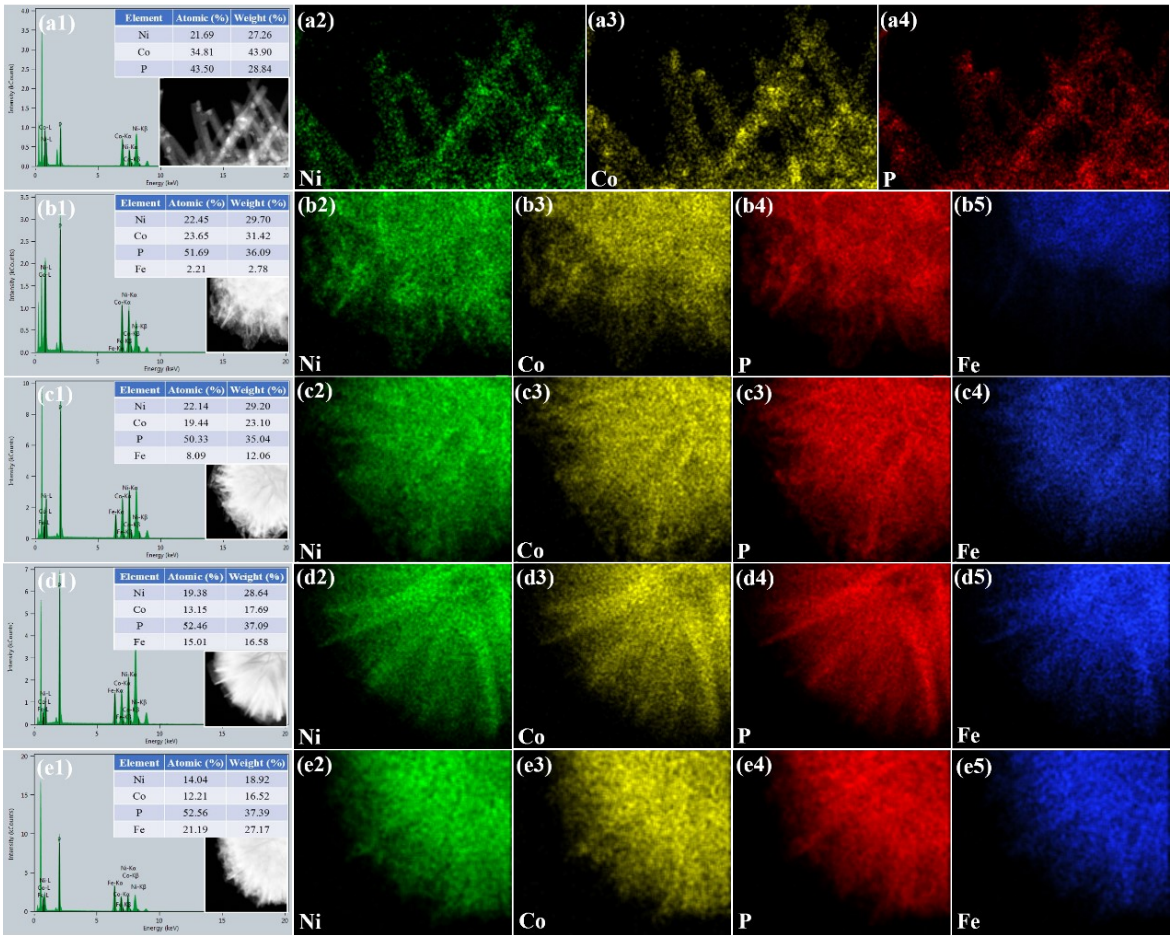

Fig. S4 (a1) EDX and (a2-a4) corresponding Ni, Co and P elemental mapping results of NiCoP powder, (b1-e1) EDX and (b2-b5, c2-c5, d2-d5, e2-e5) corresponding Ni, Co, P and Fe elemental mapping results of Fe-NiCoP-4% powder, Fe-NiCoP-6.25% powder, Fe-NiCoP-12.5% powder and Fe-NiCoP-25% powder samples.

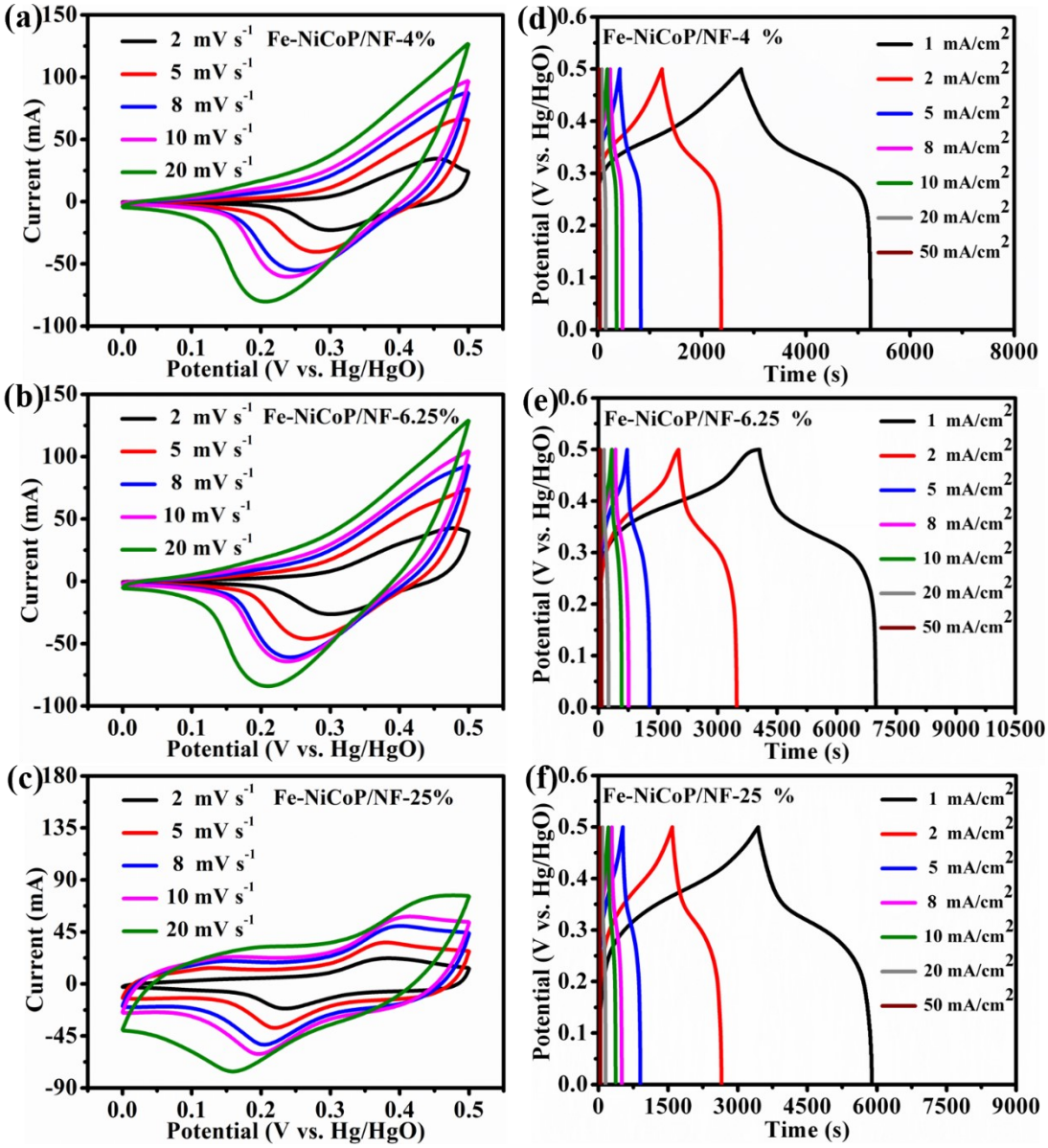

Fig. S5 (a-c) CV curves and (d-f) GCD curves of Fe-NiCoP/NF-4%, Fe-NiCoP/NF-6.25% and Fe-NiCoP/NF-25% electrodes.

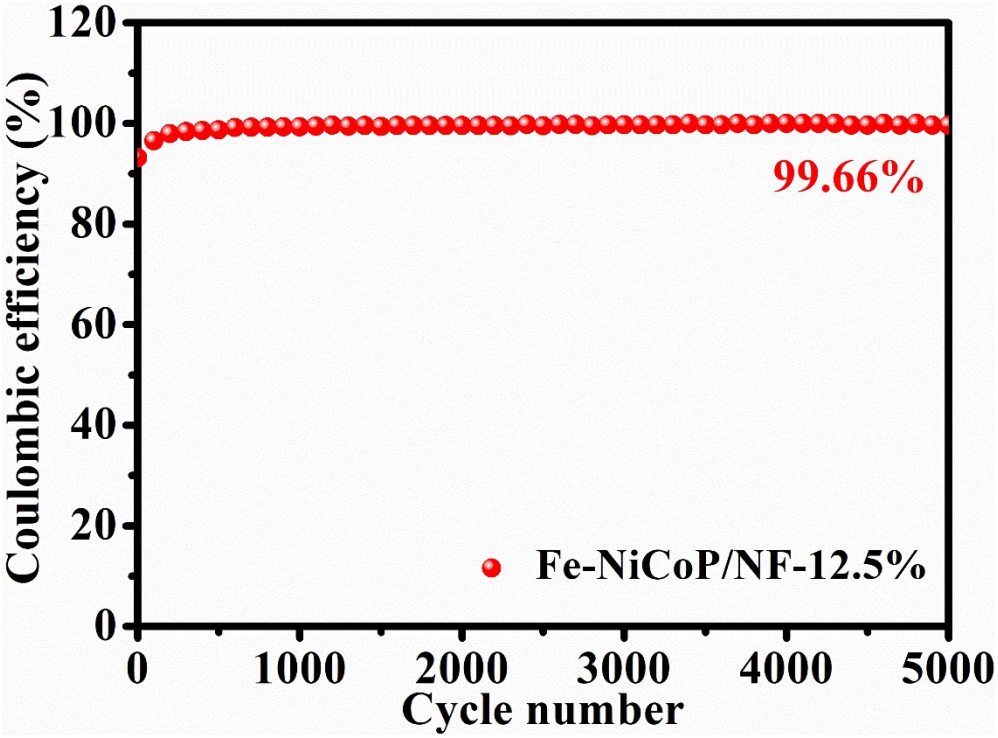

Fig. S6 Coulombic efficiency of Fe-NiCoP/NF-12.5 % electrode at 20 mA cm^{-2}.

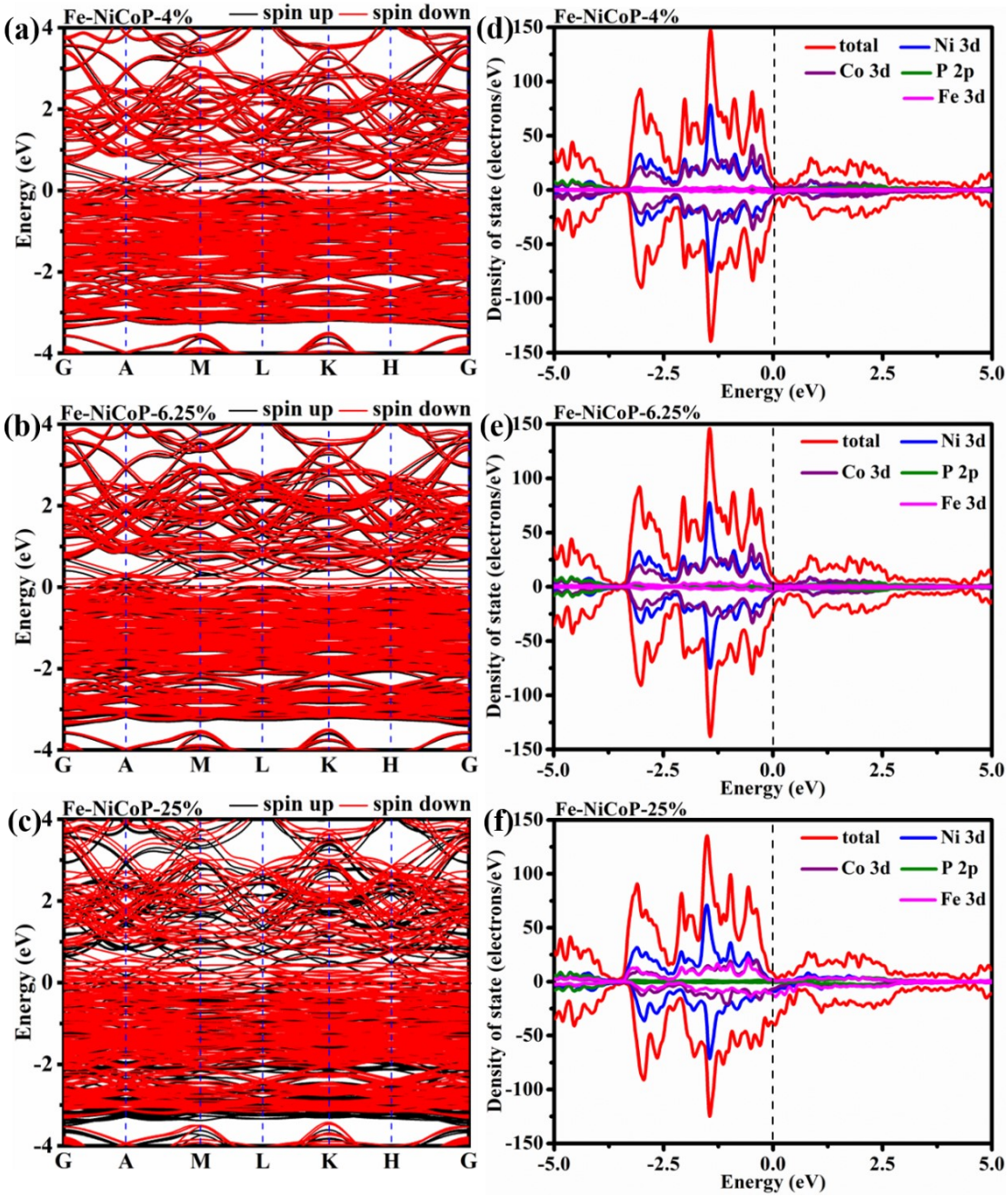

Fig. S7 (a-c) band structures and (d-f) the corresponding DOS of Fe-NiCoP-4%, Fe-NiCoP-6.25% and Fe-NiCoP-25% samples.

Table S1 Comparison of electrochemical performance for recently reported NiCoP electrode materials of supercapacitors

Samples	Loading mass	Specific capacitance	Rate performance	Cycling stability	Ref.
Fe-NiCoP/NF-12.5% nanosheets	2-4 mg cm^{-2}	9.93 F cm^{-2} (1 mA cm^{-2})	82.58% (1-50 mA cm^{-2})	95.72% (20 mA cm^{-2}, 5000 cycles)	This work
Mn-CoP/NF nanowire	6.6 mg cm^{-2}	8.66 F cm^{-2} (1 mA cm^{-2})	52.19% (1-50 mA cm^{-2})	82.1% (50 mA cm^{-2}, 2000 cycles)	Ref. [1]
O-doped NiCoP	5.07 mg cm^{-2}	3457 mC cm^{-2} (1 mA cm^{-2})	82% (1-10 mA cm^{-2})	66% (10 A g^{-1}, 3000 cycles)	Ref. [2]
NiCoP@NiCo-LDH	2.4 mg cm^{-2}	4.68 F cm^{-2} (1 mA cm^{-2})	89.3% (1-20 mA cm^{-2})	81.1% (20 mA cm^{-2}, 5000 cycles)	Ref. [3]
P-(Ni,Co)Se_2	~ 4 mg cm^{-2}	3.02 C cm^{-2} (2 mA cm^{-2})	86.42% (2-30 mA cm^{-2})	80.1% (20 mA cm^{-2}, 3000 cycles)	Ref. [4]
3D NiCoP@$MoSe_2$	2.5 mg cm^{-2}	5.61 F cm^{-2} (1 mA cm^{-2})	79.2% (1-40 mA cm^{-2})	91.9% (20 mA cm^{-2}, 8000 cycles)	Ref. [5]
NiCoP/NC	1.5 mg cm^{-2}	6.22 F cm^{-2} (1 A g^{-1})	70% (1-10 A g^{-1})	95% (20 A g^{-1}, 5000 cycles)	Ref. [6]
NiCoP/NF	—	9.2 F cm^{-2} (2 mA cm^{-2})	64.89% (2-50 mA cm^{-2})	67% (50 mA cm^{-2}, 2000 cycles)	Ref. [7]

Co-Fe-Mn phosphide	0.35 mg cm^{-2}	4.36 F cm^{-2} (2 mA cm^{-2})	65.37% (2-20 mA cm^{-2})	100% (20 mA cm^{-2}, 5000 cycles)	Ref. [8]
$CoNi_2S_4$/E-NZP@CW	—	8.9 F cm^{-2} (4 mA cm^{-2})	59.4% (4-80 mA cm^{-2})	93.4% (20 mA cm^{-2}, 7000 cycles)	Ref. [9]
Ni_xP/NF	4.4 mg cm^{-2}	1.68 F cm^{-2} (2 mA cm^{-2})	66.3% (2-20 mA cm^{-2})	110.9% (20 mA cm^{-2}, 4000 cycles)	Ref. [10]
CF@NiCoNiPC	1.68 mg cm^{-2}	1.76 F cm^{-2} (5 mA cm^{-2})	63.8% (5-30 mA cm^{-2})	86% (30 mA cm^{-2}, 4000 cycles)	Ref. [11]
Ni-P@NiCo LDH	3.37-3.74 mg cm^{-2}	12.9 F cm^{-2} (5 mA cm^{-2})	49.6% (5-100 mA cm^{-2})	96% (40 mA cm^{-2}, 10000 cycles)	Ref. [12]
NiCoP/NF	16.7 mg cm^{-2}	19.9 F cm^{-2} (50 mA cm^{-2})	49.8% (20-100 mA cm^{-2})	92% (50 mA cm^{-2}, 2000 cycles)	Ref. [13]
FeCoP@NiCoP/CC	2.2 mg cm^{-2}	973.0 C g^{-1} (1 A g^{-1})	84.3% (1-20 A g^{-1})	84.7% (5 A g^{-1}, 5000 cycles)	Ref. [14]

Table S2 The ion diffusion coefficient values for NiCoP/NF and Fe-NiCoP/NF-x% electrodes

Samples	diffusion coefficients (D, $cm^2\ s^{-1}$)
NiCoP/NF electrode	$1.88*10^{-9}$
Fe-NiCoP/NF-4% electrode	$5.20*10^{-9}$
Fe-NiCoP/NF-6.25% electrode	$2.97*10^{-9}$
Fe-NiCoP/NF-12.5% electrode	$5.42*10^{-9}$
Fe-NiCoP/NF-25% electrode	$1.28*10^{-9}$

Reference

1 G. Zhu, L. Yang, W. Wang, M. Ma, J. Zhang, H. Wen, D. Zheng and Y. Yao, *Chem Commun (Camb)*. 2018, **54**, 9234-9237.

2 J. Liu, X. Deng, S. Zhu, N. Zhao, J. Sha, L. Ma and F. He, *Electrochim. Acta*. 2021, **368**, 137528.

3 X. Gao, Y. Zhao, K. Dai, J. Wang, B. Zhang and X. Shen, *Chem. Eng. J*. 2020, **384**, 123373.

4 Q. Zong, Y. Zhu, Q. Wang, H. Yang, Q. Zhang, J. Zhan and W. Du, *Chem. Eng. J*. 2020, **392**, 123664.

5 X. Gao, L. Yin, L. Zhang, Y. Zhao and B. Zhang, *Chem. Eng. J*. 2020, **395**, 125058.

6 P.A. Shinde, M.F. Khan, M.A. Rehman, E. Jung, Q.N. Pham, Y. Won and S.C. Jun, *CrystEngComm*. 2020, **22**, 6360-6370.

7 M. Kong, Z. Wang, W. Wang, M. Ma, D. Liu, S. Hao, R. Kong, G. Du, A.M. Asiri, Y. Yao and X. Sun, *Chemistry*. 2017, **23**, 4435-4441.

8 R. Niu, G. Wang, Y. Ding, S. Tang, X. Hu and J. Zhu, *J. Mater. Chem. A*. 2019, **7**, 4431-4437.

9 S. Shahrokhian and L. Naderi, *The Journal of Physical Chemistry C*. 2019, **123**, 21353-21366.

10 X. Cao, D. Jia, D. Li, L. Cui and J. Liu, *Chem. Eng. J*. 2018, **348**, 310-318.

11 P. Sun, M. Qiu, J. Huang, J. Zhao, L. Chen, Y. Fu, G. Cui and Y. Tong, *Chem. Eng. J*. 2020, **380**, 122621.

12 J. Xing, J. Du, X. Zhang, Y. Shao, T. Zhang and C. Xu, *Dalton Trans*. 2017, **46**, 10064-10072.

13 C. Zhou, T. Gao, Y. Wang, Q. Liu and D. Xiao, *Appl. Surf. Sci*. 2019, **475**, 729-739.

14 L. Wan, Y. Wang, Y. Zhang, C. Du, J. Chen, M. Xie, Z. Tian and W. Zhang, *J. Power Sources*. 2021, **506**, 230096.